minerals

*Article*

# Sono- and Zeolite-Assisted Electrocoagulation for Compost Wastewater Treatment: Does Ultrasound Power Make a Difference?

**Nediljka Vukojević Medvidović *, Ladislav Vrsalović, Sandra Svilović, Senka Gudić and Ivona Čule**

Faculty of Chemistry and Technology, University of Split, Ruđera Boškovića 35, 21000 Split, Croatia; ladislav@ktf-split.hr (L.V.); sandra@ktf-split.hr (S.S.); sgudic@ktf-split.hr (S.G.); icule@ktf-split.hr (I.Č.)
* Correspondence: nvukojev@ktf-split.hr; Tel.: +385-21-329-452

**Abstract:** This study builds on previous research that investigated the triple hybrid wastewater treatment system combining electrocoagulation (EC), zeolite (Z), and ultrasound (US), and it examines the effects of different ultrasonic powers on compost wastewater treatment by analysing several process parameters. In the first part, two levels of US power intensity, corresponding to 20% and 100% of intensity, with and without zeolite addition, were investigated on three different electrode materials. Although satisfactory chemical oxygen demand (COD) reduction was obtained (81.42%–88.90%), better results were obtained for Al and Zn electrodes at 20% US power intensity, while for Fe better resulted were obtained at 100% US power intensity. Deteriorations of the anodic and cathodic surfaces, which were analysed using optical microscope images at 50× and 200× magnification, are generally less pronounced at higher US power intensities. Energy consumption in the range of 3.86–18.78 kWh/m$^3$ showed an increased sequence—Fe < Zn < Al. In the second part, Taguchi optimisation was used to study the influence of US intensity (0%, 20%, 100%), the electrode materials (Al, Fe, or Zn), contact time (10, 20, and 30 min), and mixing speed (150, 250, 350 rpm) on COD decrease, electrode consumption, settling velocity, and voltage (power) consumption. The result shows that increased US power enhances COD reduction, electrode mass preservation, and voltage while decreasing the settling velocity.

**Keywords:** ultrasound power intensity; sono- and zeolite-assisted electrocoagulation; electrode materials; electrode light microscopic analysis; electrode deterioration

**Citation:** Vukojević Medvidović, N.; Vrsalović, L.; Svilović, S.; Gudić, S.; Čule, I. Sono- and Zeolite-Assisted Electrocoagulation for Compost Wastewater Treatment: Does Ultrasound Power Make a Difference? *Minerals* **2024**, *14*, 1190. https://doi.org/10.3390/min14121190

Academic Editor: Yijun Cao

Received: 28 September 2024
Revised: 7 November 2024
Accepted: 20 November 2024
Published: 22 November 2024



## 1. Introduction

Water is one of the simplest and most abundant substances in nature, and it is necessary to maintain life on Earth. Industry, agriculture, and urbanisation generate large quantities of wastewater with a very complex composition that must be treated to be reused or safely released into the environment. For this reason, great importance is attached today to developing efficient and economical wastewater treatment processes [1]. EC is recognised as an effective and environmentally friendly technology for wastewater treatment because the investment costs are relatively low (small size of the equipment used), the energy required can be obtained from renewable sources, the use of chemicals can be avoided (except for the addition of electrolytes to increase electrical conductivity and reduce resistance), and a smaller amount of sludge is produced compared to classical coagulation [2,3]. EC is actually the intentional corrosion of sacrificial anodes caused by the passage of electricity, which releases metal–ion coagulants and forms corresponding hydroxides and other monomeric, polymeric, and hydroxo complexes. The electrocoagulants formed further destabilise contaminants in the wastewater solution, allowing for their agglomeration and easier separation by sedimentation or flotation (aided by the resulting gases formed at the cathode and anode). The stability of EC processes depends largely on the pH of the solution and the electrode potential, for which Pourbaix diagrams (potential-pH diagrams) provide basic information on the possible electrode reaction types and species formed [4–6]. However, the formed hydroxocomplexes can contribute to the formation of layers on the electrode surface, which leads to fouling and passivation [7,8]. The passive layer also leads to slower current flow through the two opposing electrodes, reducing coagulant production and contaminant removal [9]. According to Yang et al. (2015) [10], the problem of the formation of the passive layer of Al or Fe electrodes can be reduced by adding sufficient amounts of chloride ions that dissolve the passive layer or by using alternating current (AC). Adding zeolite particles to the solution and their mixing can help clean the surface layers formed, reduce fouling and passivation, and uniformly dissolve the anode [6]. Due to the specific spatial structure of aluminosilicates, zeolites also act as ion exchangers and adsorbents for various cations and organic pollutants from solutions, while their modified form is also effective in removing anions [11–14]. Additionally, new research has also confirmed the use of natural zeolite as a coagulant for the treatment of palm oil mill effluent [15], slaughterhouse wastewater [16], and oil recovery wastewater from polymer flooding [17]. Recently, the ultrasonic field is combined with electrocoagulation to achieve efficient wastewater treatment and reduce electrode passivation. The propagation of acoustic waves in a liquid medium causes the phenomenon of cavitation. According to Moradi et al. (2020), ultrasonic waves break the passive layer formed on the electrode surface and generate large amounts of radical species that remove pollutants by creating high-pressure points in the solution during the cavitation effect [11].

Only a few authors have investigated the effect of US power intensity on the efficiency of EC treatment. Li et al. (2013) found that phosphorus removal efficiency increased with increasing US from 1 to 4 $W/cm^2$ but decreased slightly at the highest US power of 5 $W/cm^2$ due to the stronger cavitation effect [12]. A horn-type sonolyzer with a frequency of 24 kHz and an amplitude of 20%–50% was used to investigate the effect of irradiation intensity on the removal of azo dyes (Congo red, methyl red, and eriochrome black T) by ultrasound-assisted electrocoagulation. The results show that the decolourization percentage was higher at a higher US amplitude intensity as the vibration intensity and, consequently, sonochemical effects increased [18]. He et al. (2016) investigated the effect of US power in the range of 0–150 W on the removal of RB19 by intermittent sono-EC with aluminium electrodes and found that the passive film became thinner with increasing US intensity, resulting in the release of more electrocoagulants [19]. According to Savun-Hekimoglu (2020), sonochemical reactions are strongly dependent on the intensity of the sound waves, so although the reaction rate increases with increasing power, the intensity cannot be increased indefinitely, and optimal values must be determined [20]. Al-Yaqoobi et al. (2021) found that ultrasound-assisted electrocoagulation technologies with two US power amplitudes (i.e., 20% and 80%) were efficient for the treatment of dairy wastewater in the first 20 min of the process, after which electrocoagulation alone was superior. When comparing the influence of two US power amplitudes, better results were obtained with a lower ultrasonic power amplitude of 20% [21]. Smoković et al. (2022) investigated US frequency in two levels (25 and 45 kHz) and US intensity in three levels (10%, 50%, 100%) for the removal of Mn, Ni, Cd, Cr, and Co. High efficiencies were achieved in the simultaneous EC-US process at 45 kHz and 100% intensity, proving that sonoelectrocoagulation is a promising alternative to conventional treatment methods for heavy-metal-contaminated water [22]. As evident from the literature reviews above, the number of papers dealing with the combination of EC and different US intensities is very limited, and they show different effects on removal efficiency, electrode passive film formation, and electrocoagulant release amount. Additionally, several authors point out that a lower ultrasonic power amplitude yields better results, suggesting the existence of a threshold point for ultrasound intensity.

A triple combination (EC, Z, and US) as a hybrid wastewater treatment process, which is carried out simultaneously and in two stages, was proposed by Svilović et al.

(2024) for the first time [23]. A continuous sound frequency of 40 kHz and an US power of 120 W were used as the ultrasound source. The results show that US support does not significantly reduce COD and turbidity compared to processes without the US. However, US support contributes to the reduction in voltage and electrode consumption.

This research contributes to the existing findings by further investigating complex hybrid triple systems based on EC + Z + US carried out simultaneously, specifically focusing on varying ultrasound power levels to treat compost wastewater. This study aims to provide a more detailed understanding of the system's feasibility and effectiveness when combining EC, Z, and US, examining multiple process parameters such as pH, temperature, turbidity, COD, electrode consumption, EC sludge, zeolite recovery, electrode surface deterioration (via light microscopy at different magnification), settling characteristics, and cost analysis. The novelty of this work lies in its comprehensive evaluation of different ultrasound power settings, using Taguchi optimisation to balance conflicting objectives and determine the optimal operational conditions. By assessing the process from multiple perspectives, we provide deeper insights into its practicality, feasibility, and cost-effectiveness for real-world applications, creating a more robust framework for hybrid wastewater treatment systems.

## 2. Materials and Methods

**Wastewater:** prepared from commercial Agro compost. Initial physico-chemical parameters of wastewater were as follows: a pH of 3.95, an electrical conductivity of 1.9 mS/cm, a turbidity of 251.67 NTU, a chemical oxygen demand (COD) of 1642.06 mg $O_2$/L and a total solids (TSs) content of 3.08 g/L.

**Electrodes:** Three different electrode materials were used: aluminium alloy series 2000 (AA2007) with aluminium and copper as dominating elements (Al = 92.58%, Cu = 3.84%); carbon steel with iron and copper dominating elements (Fe = 98.27%, Cu = 1.17%); and commercial zinc sacrificial electrodes with zinc and aluminium dominating elements (Zn = 99.31%–99.76%, Al = 0.1%–0.5%). A more detailed chemical composition of electrodes was published previously [24].

**Synthetic zeolite (SZ):** purchased from Alfa Aesar, marked as NaX, with density at 293 K equals $\varrho = 1.1$ g cm$^{-3}$. The diffraction pattern confirms that it belongs to the Faujasite (FAU) family. The powder X-ray diffractometer (PXRD) and SEM-EDS were published previously [25]. The zeolite was crushed and sieved, and granulation < 40 μm was used in this study.

**Hybrid processes:** Lab electrochemical cell (500 mL) with electrodes pair, immersed in an ultrasonic bath Agrolab DU100 (ARGO LAB, Carpi, Italy) of 40 kHz and 240 W of power with adjustable power intensity regulation on five levels, was used to investigate the influence of two levels of US power intensity (with level 1 and 5 that correspond to 20% and 100% of intensity). For this purpose, three different hybrid processes were conducted at three different electrode materials: EC combined with synthetic zeolite (ECZ), EC combined with synthetic zeolite and 20% of US intensity (ECZ-USInt-1), and EC combined with zeolite and 100% of US intensity (ECZ-USInt-2). The hybrid treatment was carried out with a current density of $i = 0.0182$ A/cm$^2$, NaCl addition of 0.5 g/L, synthetic zeolite addition of 15 g/L, an electrode spacing of 3 cm, mixing speed of 250 rpm, for 30 min, and without modifying the original pH values. A summary of the conducted experiments and their corresponding settings is provided in Table 1.#

*A comparative analysis* was conducted on the physico-chemical parameters of pH, temperature, chemical oxygen demand (COD), turbidity, total mass of zeolite and EC sludge, and voltage and current consumption for each process.

*The electrode mass differences* were monitored using the weighing technique.

*The electrode surface* was analysed using a light microscope MXFMS-BD, Ningbo Sunny Instruments Co. (Yuyao City, China) with a 50× and 200×magnification. The microscope was equipped with a Canon EOS 1300D digital camera (Ōita, Japan) for taking pictures of the surface.

*The settling test* of the suspensions after the implementation of the hybrid processes was carried out using the Kynch standard batch-settling test [26].

**Table 1.** Summary of the conducted experiments and their corresponding settings.

| Exp Mark | Electrode Materials | Hybrid Process Type | US Intensity, % |
|---|---|---|---|
| A1 | Al | ECZ | - |
| A2 | Al | ECZ-USInt-1 | 20 |
| A3 | Al | ECZ-USInt-2 | 100 |
| A4 | Fe | ECZ | - |
| A5 | Fe | ECZ-USInt-1 | 20 |
| A6 | Fe | ECZ-USInt-2 | 100 |
| A7 | Zn | ECZ | - |
| A8 | Zn | ECZ-USInt-1 | 20 |
| A9 | Zn | ECZ-USInt-2 | 100 |

**Optimisation by Taguchi:** Underneath the Taguchi approach are the basic concepts of the orthogonal array for experimental design and the signal-to-noise ratio (S/N) for quality evaluation. The orthogonal array consists of adjustable factors and experimental combinations. The experiments in this work were designed based on Taguchi's L9 orthogonal array, as outlined in Table 2. The L9 consists of nine rows that define the number of experiments and four columns that reflect the controllable variables. The influence of US intensity (0%, 20%, and 100%), electrode materials (Al, Fe, or Zn), contact time (10, 20, and 30 min), and mixing speed (150, 250, and 350 rpm) on COD decrease, electrode consumption, settling velocity, and voltage (power) consumption were studied. It is evident that each controllable factor is associated with three test levels.

**Table 2.** Design of the experiments using Taguchi L9.

| Exp. Mark | Hybrid Process Type | Controllable Factors (Mark) | | | |
|---|---|---|---|---|---|
| | | US Intensity (US), % | Electrode Materials (M) | Mixing Speed (N), rpm | Reaction Time (t), min |
| B1 | ECZ | 0 | Al | 150 | 10 |
| B2 | ECZ | 0 | Fe | 250 | 20 |
| B3 | ECZ | 0 | Zn | 350 | 30 |
| B4 | ECZ-USInt-1 | 20 | Al | 250 | 30 |
| B5 | ECZ-USInt-1 | 20 | Fe | 350 | 10 |
| B6 | ECZ-USInt-1 | 20 | Zn | 150 | 20 |
| B7 | ECZ-USInt-2 | 100 | Al | 350 | 20 |
| B8 | ECZ-USInt-2 | 100 | Fe | 150 | 30 |
| B9 | ECZ-USInt-2 | 100 | Zn | 250 | 10 |

The Taguchi approach employs three quality characteristics: the larger-the-better, nominal-the-best, and smaller-the-better. As the objective of this work was to determine the best settings for achieving the greatest decrease in COD and the highest settling speed while minimising electrode and voltage energy consumption, the larger-the-better and smaller-the-better quality characteristics were used, respectively. The quality characteristics are expressed by employing Equations (1) and (2) [24].

$$S/N_{LB} = -10 \log \frac{\sum_{i=1}^{n} \frac{1}{y_i^2}}{n} \quad (1)$$

$$S/N_{SB} = -10 \log \frac{\sum_{i=1}^{n} y_i^2}{n} \quad (2)$$

where S/N is the signal-to-noise ratio, LB is the larger-the-better subscript, SB is the smaller-the-better superscript, n is the number of repetitions conducted under the same conditions, and y is the result obtained from the experiment. Along with the $S/N_{LB}$ and $S/N_{SB}$, the percentage of contribution and range were calculated for each level of each controllable element to enhance process analysis.

## 3. Results

### *3.1. Treatment Efficiency of ECZ and Sono-ECZ Hybrid Process at Different Electrode Materials and US Intensity*

The combination of electrocoagulation and ultrasound as a hybrid process is based on the dissolution of positively charged metal ions on electrodes, which neutralise the repulsive forces between the particles, attract them, and form flocs. At the same time, the ultrasonic cavitation produces highly reactive and non-specific radicals, which lead to additional degradation of the contamination [27]. In addition, while passing through the medium, ultrasound acts on contaminants through mechanical effects (vibration and sound flow), thermal effects, and cavitation effects [28]. However, if the ultrasound intensity is higher than the optimal value, the degradation of organic matter may also decrease [29]. To gain insight into the efficiency of the treatment of the ECZ and sono-ECZ hybrid process, it is useful to look not only at the final values of the parameters that indicate the percentage of removal but also at the changes in the classical parameters in the solution such as pH, temperature, and electrical conductivity, as their variation can provide much more information about the course of the process, the causes, and the consequences.

The change in pH and temperature during compost wastewater treatment by ECZ and sono-ECZ hybrid processes at different US intensities and electrode materials are compared in Figure 1.

The change in pH values and temperature show an increasing trend for all ECZ and sono-ECZ hybrid processes but with different intensities. The curve of pH change in the sono-ECZ process of different US power intensities almost overlaps with the ECZ curve for each material, indicating that the sonication effect does not have a significant influence on pH change. However, the increase in pH (which is mostly attributed to the generation of $OH^-$ ions dissociated from water at the cathode) [23,24] depends on electrode materials and follows the sequence Al < Fe < Zn.

Regarding the temperature change, for the hybrid sono-ECZ, a slightly higher temperature rise can be observed when applying the intensity of level 2. This can be related to the higher temperature rise in the ultrasonic bath, where an increase up to 32–33.1 °C is recorded depending on the electrode material. According to Asgharian et al. (2016) [29] and Al-Yaqoobi et al. (2021) [21], the temperature of the solution in the sono-EC process increases more with increasing amplitude of the ultrasonic power due to the high temperature of the core and the surface of the cavitation bubbles. According to Wang et al. (2019), with the increase in the US intensity, the collapse of cavitation bubbles achieves more violently, resulting in higher temperature and higher pressure. On the other hand, the degradation of organic matter also decreases if the intensity is higher than the optimal value [30]. In addition, due to the higher temperature rise during the sono-ECZ process, the generation of the dissolved electrode ions increases, while the probability of metal hydroxide formation can be reduced as the acoustic waves act on colloidal hydroxides and damage the adsorption layer on the surface of the colloidal particles [31]. At the same time, it should be kept in mind that increasing the temperature of the compost wastewater can trigger additional biodegradation of the organic compounds.

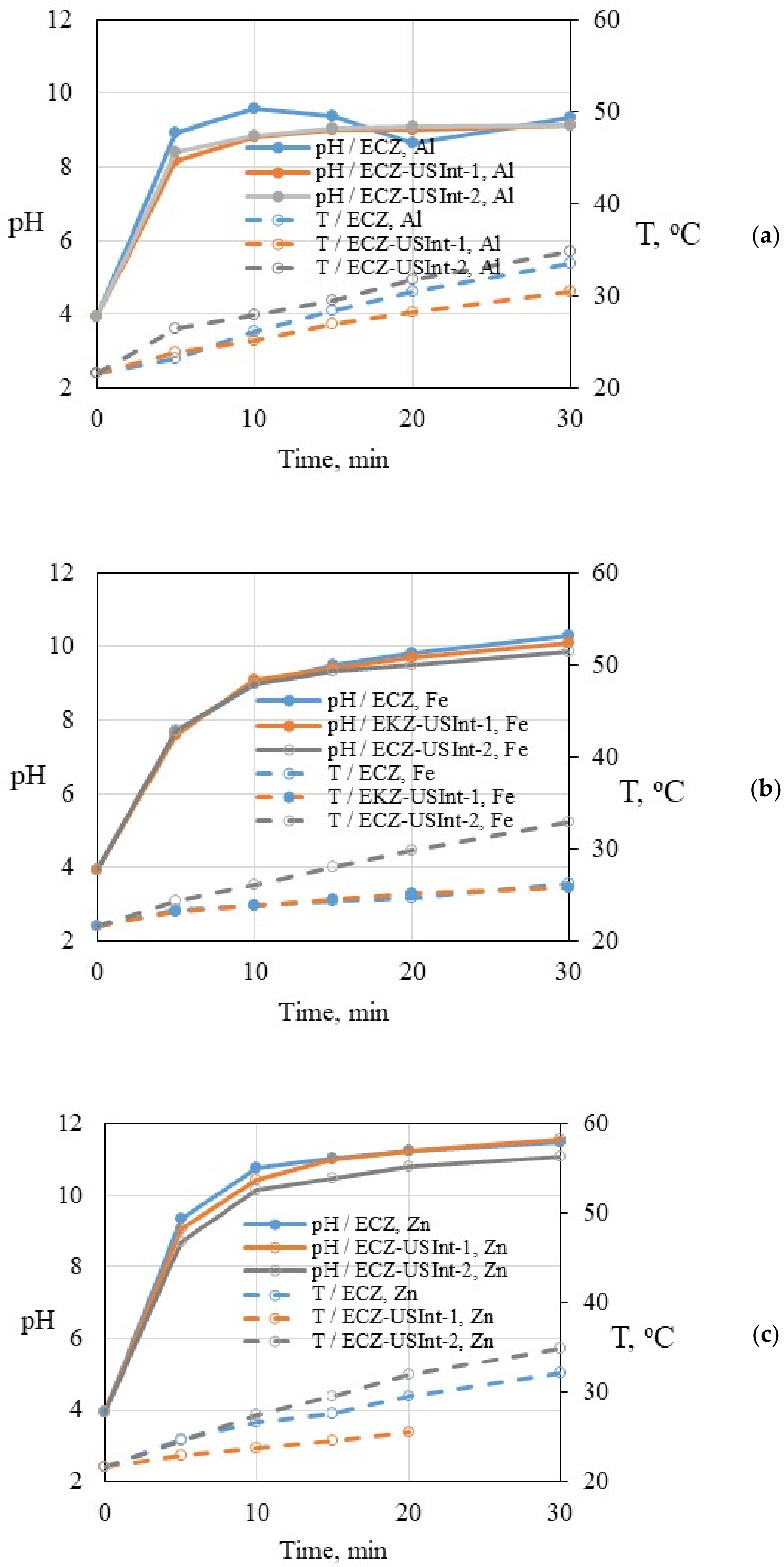


**Figure 1.** Influence of US power intensity on change in pH values and temperature during compost wastewater treatment by ECZ and sono-ECZ hybrid processes for (**a**) Al electrode; (**b**) Fe electrode,

and (**c**) Zn electrode. (Note: initial pH value and temperature were $pH_0$ = 3.95 and $T_0$ = 21.7 °C, respectively).

Table 3 summarises the parameters measured during each ECZ and sono-ECZ hybrid processes at different US intensity and electrode materials. The calculation of COD and turbidity decrease (%) was performed according to the following equation:

$$\text{COD/turbidity decrease} \quad (\%) = \frac{c_I - c_F}{c_I} \cdot 100 \tag{3}$$

where $c_I$ and $c_F$ are the initial and final values of COD of turbidity in solution (in mg $O_2$/L or NTU units).

**Table 3.** Parameters measured during each ECZ and sono-ECZ hybrid process.

| Exp Mark | COD Decrease, % | Turbidity Decrease, % | TS, g/L |
|---|---|---|---|
| ECZ, Al | 87.21 | 67.80 | 2.055 |
| ECZ-USInt-1, Al | 86.49 | 73.95 | 1.935 |
| ECZ-USInt-2, Al | 86.97 | 7.62 | 2.040 |
| ECZ, Fe | 85.28 | 98.45 | 2.015 |
| ECZ-USInt-1, Fe | 85.52 | 81.94 | 2.030 |
| ECZ-USInt-2, Fe | 88.90 | 97.95 | 2.030 |
| ECZ, Zn | 81.90 | 53.11 | - |
| ECZ-USInt-1, Zn | 82.63 | 76.52 | 2.015 |
| ECZ-USInt-2, Zn | 81.42 | −9.47 | 2.245 |

The results in Table 3 show that increasing the US power intensity does not increase the COD reduction for the Al electrode (87.21% to 86.49%), while the opposite is achieved for the Fe electrode (the percentage COD reduction increases from 85.28% to 88.90% when the US intensity is increased). With the Zn electrode, the best results are achieved when using the US power intensity level 1, which equals 82.63%. In their study, Al-Yaqoobi et al. (2021) [21] found that the use of ultrasound along with electrochemical (EC) with aluminium (Al) electrodes has a detrimental effect on the colloids of aluminium hydroxide. This effect leads to the easy desorption and return of pollutants that are adsorbed on the aluminium hydroxide to the solution. Namely, they also found that process duration when ultrasound is applied can have either a positive or negative impact. The influence of microbubbles produced by sonication during the first 20 min of the treatment is beneficial due to the enhanced floc flotation. However, the subsequent reduction in the removal efficiency in the ECZ-US system most likely stems from the impact of ultrasound on colloidal hydroxides and damage of the adsorption layer at the surface of the colloidal particle, during which desorption of the pollutants can occur [21]. However, this was not observed at the Fe electrode, which agrees with the previous study [31]. According to Oznoyar et al. (2020), the $Al(OH)_3$ flocks are more affected than $Fe(OH)_3$ due to the larger specific surface area [32]. As far as we know, there has been no investigation of sono-EC with Zn electrodes.

Although all hybrid processes achieve a substantial reduction in COD (ranging from 81.42% to 88.90%), the final COD values in solution (ranging from 182.25 to 305.07 mg $O_2$/L) still exceed the maximum allowable limit of 125 mg $O_2$/L [33]. This suggests that further treatment processes will be necessary before these solutions can be discharged into the sewage system.

Regarding the decrease in turbidity, the best results were obtained with the Fe electrode, without US (98.45%) and with 100% US power intensity (97.95%). With Al and Zn electrodes, the best results are obtained with 20% of US power intensity (73.95% and 76.52%, respectively). However, when applying 100% of US power intensity at the Zn electrode, it negatively affected the reduction in turbidity, resulting in an increased final turbidity value. Thus, the percentage of turbidity decrease achieved negative value (−9.47%).

In terms of the chemical components removed from compost wastewater, it is well known that compost wastewater is typically polluted with soluble and particulate organic matter, as well as nutrients, indicating a high organic content and complex chemical composition [34]. The initial organic matter content, as indicated by COD values, primarily consists of humin, humic acids, and fulvic acids, which are present in both dissolved and colloidal forms in compost leachate [34,35]. Mullane et al. (2015) also confirmed that dissolved organic compounds in compost leachate from bioretention systems primarily consist of aliphatic and aromatic components typical of fulvic and humic acids [36]. The difference in COD between humic acid and fulvic acid arises from the strength of the chemical bonds within each compound, resulting in a higher COD for humic acid than for fulvic acid. In this regard, the removal of humic acid from solution has been more extensively studied [35]. It is also known that the removal mechanism of humic acid by EC is related to pH, as it affects both the in situ formation of electrocoagulant hydrolysis species and the surface charge of humic acid molecules [37–39]. S. Kourdali et al. (2014) proposed two mechanisms for humic acid removal during EC treatment with Al electrodes, based on neutralisation–precipitation effects or sweep coagulation/floc formation. Additionally, FTIR spectra and HPLC analyses show that the humic acid molecules did not undergo any structural modifications during EC removal [39]. According to Mahvi et al. (2009), ultrasonic treatment alone is not an efficient method for the degradation of humic substances [40]. However, when US of different frequencies and intensities is combined with EC, humic acid removal can result in either synergistic or antagonistic effects. Our results indicate that this effect also depends on the electrode material. Increasing the intensity of US on Al electrodes results in an antagonistic effect. Similar findings were reported by Asgharian et al. (2016), where the combined use of EC and US led to lower humic acid removal, as the US waves caused coagulated humic acid to dissolve back into the solution, thereby reducing overall removal efficiency [29]. By contrast, using Fe electrodes produced the opposite effect, while with Zn electrodes, the threshold was reached at 20% US power intensity. The turbidity removal results followed a pattern similar to COD reduction.

Values of TS after the application of ECZ and sono-ECZ with different US intensities and electrode materials slightly oscillate in the range of 1.935–2.245 g/L, depending on the experimental condition. However, they are generally lower compared to initial TS values of compost wastewater of 3.08 g/L.

In their study, Roy et al. (2018) [34] compare different technologies for the treatment of compost leachate, ranging from biological (biofilters, anaerobic bioreactors with potential for biogas production, membrane bioreactors (MBRs), and wetlands), physico-chemical (coagulation–flocculation, electrocoagulation, flotation, and filtration) and advanced wastewater treatment technologies (focusing on advanced oxidation processes (AOPs) with ozone used alone or in combination with $H_2O_2$ or persulfate, Fenton, Photo-Fenton and UV/$TiO_2$). Compared to the results obtained in this study, where COD reduction is between 81.42% and 88.90%, several other technologies achieve better results. In the first place, membrane technologies (ultrafiltration (UF)/nanofiltration (NF), coagulation/NF, lime precipitation/UF/reverse osmosis (RO), and microfiltration/UF/RO) achieve a COD reduction of more than 95%, even with a very high initial organic load of feed wastewater. A similar result was achieved by applying electrocoagulation–flocculation with Al electrodes, where 96% COD reduction was achieved at a very high initial COD load (14.5 g/L). The highest COD reduction and ammonia nitrogen removal (99.7% and 99.9%, respectively) were achieved with the MBR configuration. Among the AOPs, the $O_3$/persulphate technology achieved the highest COD reduction of 87%. It could be observed that technologies combining EC, Z, and US are less efficient than some other technologies. However, in the final application, the appropriate technology selection is based on the percentage of COD reduction and other factors, such as overall cost and the simplicity of design and operation. In this respect, technologies that propose a triple combination of EC, Z, and US still have great potential.

### *3.2. Analysis of Electrode Mass Change and EC Sludge Recovery*

Before and after each hybrid process, the mass of the electrodes was measured. The acquired results were utilised to compute electrode consumption through a change in mass. Figure 2a shows comparisons of electrode consumption values for each hybrid process.

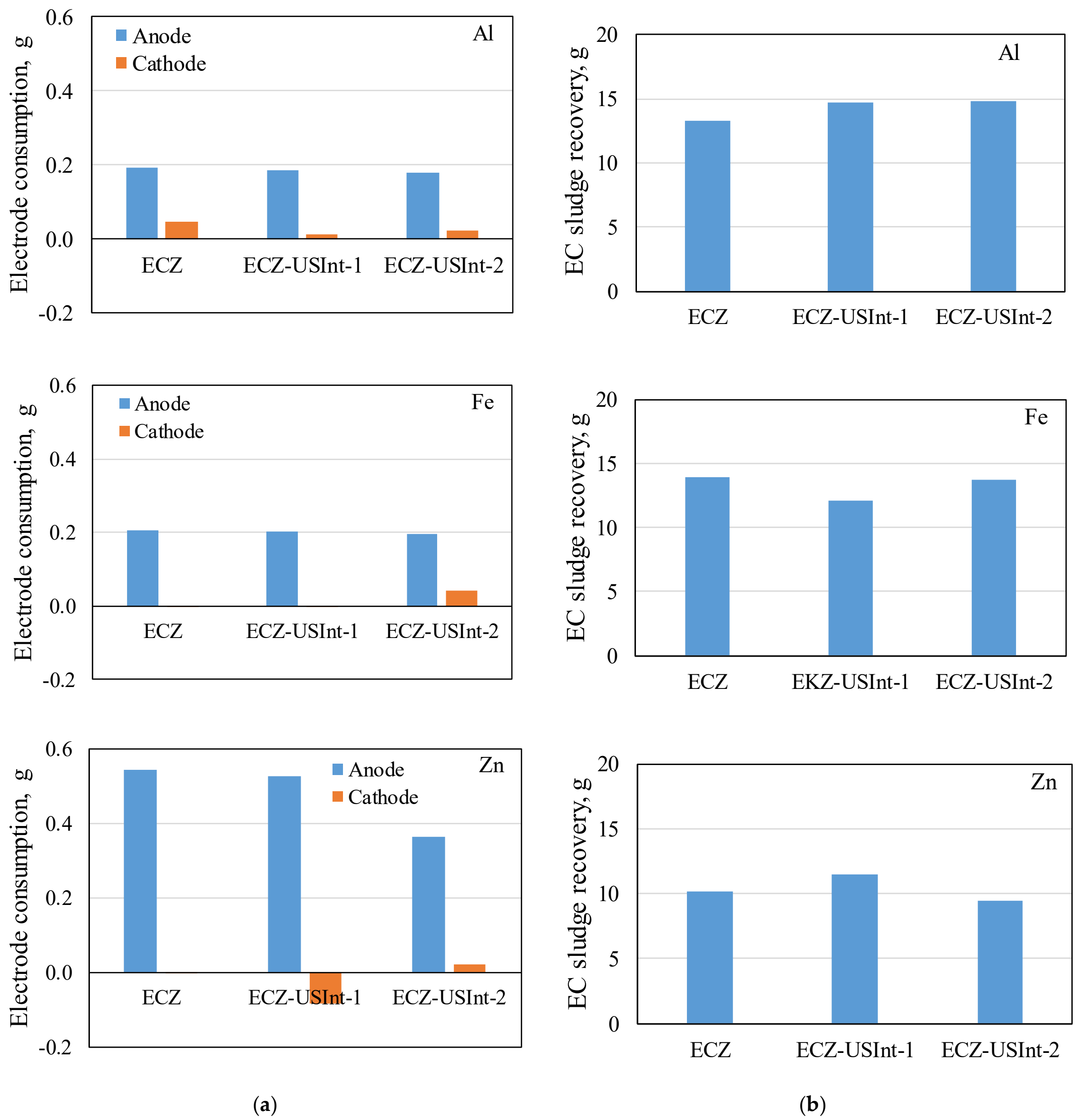


**Figure 2.** Influence of US power intensity and electrode materials on (**a**) electrode consumption; (**b**) EC sludge recovery during compost wastewater treatment by ECZ and the sono-ECZ hybrid process.

The results in Figure 2a show that an increase in US power intensity only slightly reduces the anode consumption made of Al and Fe, while at the Zn electrode, anode consumption is more reduced. Cathode mass changes (increase and decrease) are also evident and dependent on applied US power intensity and electrode materials. More about surface changes on electrodes will be discussed in Section 3.3: *Light Microscopic Analysis of the Electrode Surface.*

Collected EC sludge includes the saturated zeolite and sludge produced during the EC process (oxide/hydroxide precipitates formed by electrocoagulation). Taking into account that 15 g/L of zeolite was added during each process and that the mass of produced EC sludge varies in the range of 0.1–1.75 g/L of treated compost wastewater [41], depending on the initial composition of the solution, the type of electrode material, and the EC working conditions, recovery of EC sludge is in the range of 52%–88%. Among electrode materials, the best EC sludge recovery is obtained with Al electrodes, and recovery increases with increasing US intensity (from 78% to 87%). The lowest recovery is with Zn electrodes (52%–66%). Applying ultrasonic (US) intensity benefits the zinc (Zn) electrode only when applied at intensity level 1, which is equivalent to 20% of the US intensity. When using Fe electrodes, increasing the intensity of ultrasonication does not improve EC sludge recovery.

### 3.3. Light Microscopic Analysis of the Electrode Surface

The results of analysing the surface of the electrodes with a light microscope at different magnifications (50× and 200×) after each process are shown in Figures 3 and 4.

In order to analyse the corrosion damage on the electrode surface in more detail, microscopic images are shown at 200× magnification in bright field and dark field mode. Dark-field obtains greater resolutions than bright-field microscopy, thus presenting the samples in greater detail.

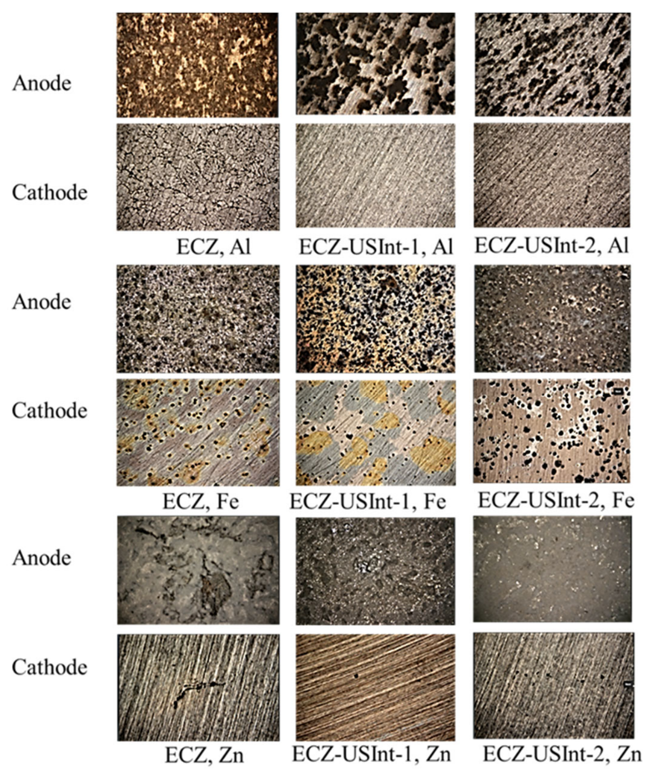


**Figure 3.** Electron microscopic surface analysis of electrodes (magnification 50×, bright field BF) after ECZ and sono-ECZ hybrid with different US power intensity and electrode materials.

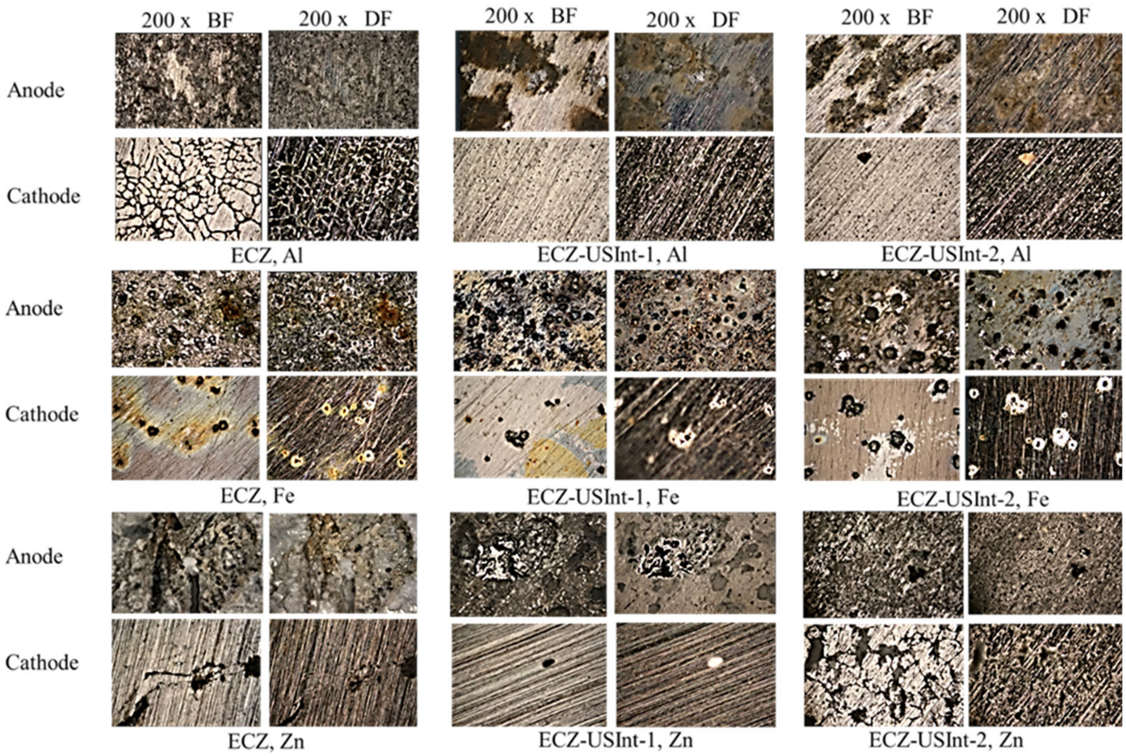


**Figure 4.** Microscopic surface analysis of electrodes surface (magnification 200×, bright field BF, and dark field DF) after ECZ and sono-ECZ hybrid with different US power intensity and electrode materials.

Optical microscope images (at 50× and 200× magnification) clearly show damage to both the anode and cathode surfaces of all electrode materials, which is generally less pronounced at different US intensities. Almost the entire surface of the Al anode was damaged during the ECZ process, and general and pitting corrosion is visible. The application of the US led to a reduction in the damage to the anode to some extent. After the ECZ process, the dendritic structure (cracked layer) of the aluminium cathode surface can be observed, which is probably the result of the cathodic reduction in organic compounds, together with the intense hydrogen evolution and the formation of $OH^-$ ions, which can chemically attack the cathode surface. With the influence of the US, the dendrite structure disappears completely.

Pitting corrosion is easily visible both on the surface of the Fe anode and cathode, as well as uniform corrosion on the anode. Brown–yellow areas around the pits indicate the formation of corrosion products from iron oxides. Higher US intensity leads to the complete disappearance of yellow areas on both electrodes, while the pitting damage is still visible, especially on the cathode. Damages on Zn anodes are highest after the ECS process, which are reduced to some extent using ultrasound.

The obtained results confirmed the hypothesis in the literature that ultrasound has a dual effect, which was attributed to different influences on the anode and the electrolyte [42,43]. On the anode, the ultrasonic vibrations promoted the desorption of the bubbles and ion migration, which led to the growth of the surface film [42–44]. This may be the reason for the slightly lower mass loss of all anodic materials in the experiments with ultrasound. However, the effect of ultrasonic cavitation in the electrolyte reduces the concentration gradient of the charged particles and intensifies the process of floccule formation [42]. This is in accordance with the obtained results, namely in the presence of ultrasound waves, when the ultrasound was focused on the electrolyte, which was attributed to the effect of ultrasonic cavitation, which reduced the concentration gradient of charged particles and inhibited mass transfer, resulting in the foaming of oppositely charged particles in the area between the electrodes [42–44], which promotes flocculation and coagulation.

### *3.4. Settling Velocity*

The results of the settling tests performed by the classical Kynch method are shown in Figure 5.

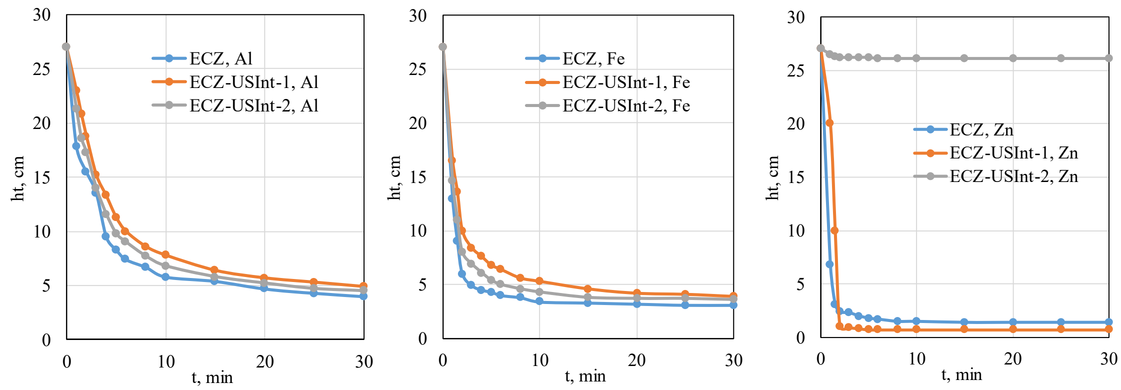


(**a**) Al electrodes (**b**) Fe electrodes (**c**) Zn electrodes

**Figure 5.** Settling curves of suspension after ECZ and sono-ECZ hybrid with different US power intensity and electrode materials.

Settling curves of suspension after hybrid processes of EC with different US intensity and electrode materials show good settling abilities (characterised by good separation of solid and liquid phases) for all experimental conditions except for the Zn electrode after application of US intensity level 2. However, the solution is very cloudy, and the percentage of turbidity decrease achieves a negative value, most likely due to floc breaking (−9.47%—see Table 4).

**Table 4.** The comparison of calculated electrode and energy cost.

| Experiment Mark | U, V | $C_{energy}$, kWh/m³ | $C_{electrode}$, kg/m³ | $C_{electrode, (Faraday)}$ kg/m³ | Operating Cost eur/m³ |
|---|---|---|---|---|---|
| ECZ, Al | 21.63 | 18.78 | 0.39 | 0.29 | 2.822 |
| ECZ-USInt-1, Al | 21.59 | 18.74 | 0.37 | 0.29 | 2.772 |
| ECZ-USInt-2, Al | 20.35 | 17.67 | 0.36 | 0.29 | 2.639 |
| ECZ, Fe | 15.37 | 5.87 | 0.41 | 0.40 | 0.977 |
| ECZ-USInt-1, Fe | 12.32 | 4.71 | 0.40 | 0.40 | 0.847 |
| ECZ-USInt-2, Fe | 10.11 | 3.86 | 0.39 | 0.40 | 0.750 |
| ECZ, Zn | 18.74 | 14.07 | 1.09 | 0.92 | 2.546 |
| ECZ-USInt-1, Zn | 20.30 | 14.78 | 1.05 | 0.92 | 2.580 |
| ECZ-USInt-2, Zn | 20.73 | 15.57 | 0.73 | 0.92 | 2.341 |

### *3.5. The Operational Cost of Sono-Assisted Zeolite-Based EC Hybrid Processes*

The operating costs of the process include all costs such as materials and energy costs, chemical reagents, waste sludge disposal, labour, maintenance, and equipment costs [45–47] As the most important parameters are electrode materials and electrical energy consumption, focus will be on its calculation, according to Equation (4):

$$\text{Operating cost} = a \times C_{energy} + b \times C_{electrode} \quad (4)$$

where $C_{energy}$, $C_{electrode}$, a, and b are energy consumption per cubic metre of wastewater ($kWh/m^3$), consumed electrode for treatment of a cubic metre wastewater ($kg/m^3$), approximate cost of materials (2.25 euro/kg Al sheet [48,49], low carbon steel 0.9 euro/kg [50], and Zn anode 1 euro/kg [51]), and electricity price at 0.1035 euro/KWh [52], respectively.

Consumption of energy is calculated according to the following (5):

$$C_{energy} = \frac{U \times I \times t}{V} \quad (5)$$

where *U*, *I*, and *t* stand for the average voltage of the EC system (*U*), electrical current intensity (*I*), and reaction time (*t*), respectively, and *V* is the volume of wastewater.

Electrode consumption is calculated from the mass lost during the EC process (Figure 2a). The results are shown in Table 4. For comparison, the table also shows the results of the theoretical material consumption calculated according to Faraday's laws.

The values of the applied current and voltage vary depending on the experimental conditions of the ECZ and sono-ECZ hybrid processes. However, by applying ultrasound with two different power levels of intensities to the Al and Fe electrodes, the voltage consumption decreases slightly, while the opposite behaviour was observed for the Zn electrodes. According to Al-Rubaiey and Al-Barazanjy (2018) [31], the applied voltage controls both the rate of coagulant dosing (in situ by dissolving the electrode) and the production and formation of bubbles and, consequently, the growth of flocs. Obviously, the situation varies depending on the electrode material.

Energy consumption is highest in experiments with Al electrodes (between 17.67 $kWh/m^3$ and 18.78 $kWh/m^3$), then with zinc electrodes (between 14.07 $kWh/m^3$ and 15.57 $kWh/m^3$), and is lowest with Fe electrodes (between 3.86 $kWh/m^3$ and 5.87 $kWh/m^3$). When different US intensities are applied, energy consumption decreases with Al and Fe electrodes, while the opposite effect is observed with Zn electrodes. As can be seen from Table 4, experiments with Zn electrodes show higher electrode consumption, while the consumption of Al and Fe is significantly lower. The total electrode material consumption of Al is higher than the theoretical value, which is a consequence of electrochemical and chemical reactions that contribute significantly to the dissolution of aluminium electrodes to generate coagulant $Al^{3+}$ in the EC process. A similar result was observed in previous findings, known as super-faradaic efficiency [46,53,54]. When using Fe and Zn electrodes, these differences are less pronounced. In the ECZ-USInt-2 experiment with a Zn electrode, the consumption of the electrode calculated from the mass lost during the EC process is 20.65% lower than the theoretical consumption of the electrode calculated according to Faraday's laws. Table 4's results demonstrate that an increase in US intensity leads to a decrease in the electrode consumption based on lost mass, regardless of the electrode material.

The efficiency and cost-effectiveness of electrocoagulation (EC) in comparison to traditional treatment methods, including chemical coagulation, have been investigated in previous studies [55,56]. Eskibalci and Ozkan (2018) evaluated the operational costs of EC with two different electrodes versus conventional coagulation methods using various coagulants for dewatering in coal preparation plants. Their findings showed that EC operating costs were 22.2% lower than those of chemical coagulation, with comparable removal efficiency [55]. Similarly, Moosavirad (2016) compared the unit costs of EC with an aluminium electrode to those of other treatment methods for grey water, demonstrating that EC was more cost-effective than both coagulation and biological treatment combined with microfiltration, UV filtration, and ozonation, or ultrafiltration [56].

It is important to note that determining the most effective technology requires comparing treatments for similar effluent types, as these vary in source, volume, pollutant concentration, and specific treatment requirements. Direct comparisons are challenging to find, and tables summarising the treatment of various wastewater types using EC and similar techniques are more commonly available. For example, Morradi et al. (2021) reviewed recent studies on pollutant removal using sono-electrocoagulation, reporting energy costs (in USD/m$^3$) ranging from 0.104 USD/m$^3$ for dispersed dye removal in synthetic wastewater to 6.28 USD/m$^3$ for COD reduction in oil tanning wastewater [11]. In this study, the calculated operating costs for sono- and zeolite-assisted electrocoagulation (expressed in EUR/m$^3$) fall within this range, from 0.750 EUR/m$^3$ to 2.822 EUR/m$^3$.

Summarising the discussion given in Sections 3.1–3.5, and taking into account the satisfied values of COD and turbidity decrease, the electrode consumption and its surface deterioration, settling abilities of suspension, and the amount of EC sludge and zeolite collected after each experiment, as well as the electricity and electrode cost, the results highlight the finding that electrocoagulation with the use of iron electrodes with 100% of ultrasound power intensity for a process duration of 30 min, rotation speed of the mixer at 250 rpm, and synthetic zeolite granulation < 40 µm is best to use.

### *3.6. Taguchi Optimisation*

As a way to optimise the coupled process of ECZ with and without ultrasound, a new series of nine experiments, shown in Table 2, were conducted to assess the impact of US intensity, electrode materials, mixing speed, and time on COD decrease, electrode consumption, settling velocity, and voltage consumption. Tables 5 and 6 present the experimental results of these studies and the values of $S/N_{LB}$ and $S/N_{SB}$ ratios calculated by Equations (1) and (2). Furthermore, the signal-to-noise ratio of each factor was also computed (S/N ratio), just as the contribution percentage (pC). The contribution percentage assists in identifying the factors that strongly influence the result of the examined process. An important role of these values is to assess the significance of the tested factors in achieving the intended outcomes of the process. The computing methods' formula is provided elsewhere [57].

**Table 5.** Average values of experimental results for Taguchi analysis.

| Experimental Conditions | COD Decrease, % | Settling Velocity, cm/min | Loss of Electrodes Mass, g | Voltage, V |
|---|---|---|---|---|
| ECZ, Al, 150 rpm, 10 min | 79.34 | 2.857 | 0.0614 | 22.05 |
| ECZ, Fe, 250 rpm, 20 min | 84.92 | 1.426 | 0.1417 | 12.05 |
| ECZ, Zn, 350 rpm, 30 min | 82.55 | 1.452 | 0.5453 | 20.7 |
| ECZ-USInt-1, Al, 250 rpm, 30 min | 87.64 | 1.177 | 0.1658 | 9.07 |
| ECZ-USInt-1, Fe, 350 rpm, 10 min | 77.58 | 0.017 | 0.0802 | 14.51 |
| ECZ-USInt-1, Zn, 150 rpm, 20 min | 78.12 | 0.025 | 0.3080 | 17.47 |
| ECZ-USInt-2, Al, 350 rpm, 20 min | 86.69 | 0.007 | 0.1294 | 16.28 |
| ECZ-USInt-2, Fe, 150 rpm, 30 min | 86.55 | 0.966 | 0.2199 | 17.12 |
| ECZ-USInt-2, Zn, 250 rpm, 10 min | 77.23 | 0.007 | 0.2077 | 18.53 |

**Table 6.** $S/N_{LB}$ and $S/N_{SB}$ ratios.

| Experimental Conditions | $S/N_{LB}$ Ratio COD Decrease | $S/N_{LB}$ Ratio Settling Velocity | $S/N_{SB}$ Ratio Loss of Electrodes Mass | $S/N_{SB}$ Ratio Voltage |
|---|---|---|---|---|
| ECZ, Al, 150 rpm, 10 min | 37.989 | 9.118 | 24.237 | −26.87 |
| ECZ, Fe, 250 rpm, 20 min | 38.580 | 3.082 | 16.973 | −21.62 |
| ECZ, Zn, 350 rpm, 30 min | 38.334 | 3.239 | 5.267 | −26.32 |
| ECZ-USInt-1, Al, 250 rpm, 30 min | 38.854 | 1.416 | 15.608 | −19.15 |
| ECZ-USInt-1, Fe, 350 rpm, 10 min | 37.795 | −35.391 | 21.917 | −23.23 |
| ECZ-USInt-1, Zn, 150 rpm, 20 min | 37.855 | −32.041 | 10.229 | −24.85 |
| ECZ-USInt-2, Al, 350 rpm, 20 min | 38.759 | −43.098 | 17.761 | −24.23 |
| ECZ-USInt-2, Fe, 150 rpm, 30 min | 38.745 | −0.301 | 13.156 | −24.67 |

| | | | | |
|---|---|---|---|---|
| ECZ-USInt-2, Zn, 250 rpm, 10 min | 37.756 | −43.098 | 13.651 | −25.36 |

The initial COD value decreases between 77.23% and 99.34%, which results in $S/N_{LB}$ ratios in the range of 37.756 to 38.854. Average settling velocity is in the range of 0.007 to 2.857, with $S/N_{LB}$ ratios of −43.098 to 9.118. The average electrode loss ranges from 0.003 to 0.069 g, and power consumption ranges from 9.07 to 22.05.

According to the data, Tables 7 and 8, ultrasound has a positive effect on COD removal (USInt-2), electrode mass (USInt-1), and voltage (USInt-1). However, the percentage of this factor's contribution to COD removal is only 5.81% in contrast to the duration of the process and electrode material with a pC of 61.00% and 29.54%, respectively. It is the same for electrode mass. pC of US usage is 0.64%, while for electrode material and time, it is 56.99% and 41.92%, respectively. These data indicate that US has a relatively minor effect on COD removal and electrode mass change. Therefore, if COD removal and electrode mass loss are targeted results of optimisation, the focus should be on the adjustment of process duration and electrode material. This has a greater influence on the voltage, and its pC is 25.64%. On settling velocity, the application of ultrasound has a negative impact, and this factor has the highest pC (48.32%).

As in previous studies, Al is the best electrode material for the treatment of wastewater with a very high organic load [6]. Regarding mixing speed, it is important to consider the benefits of homogenising the reaction mixture and enhancing ion mobility by solution mixing, as well as the drawbacks, which manifest as the collapse of the flocs [58]. Despite using higher mixing speeds compared to prior studies (50–250 rpm), this work proved that a speed of 150 rpm generally provides an acceptable compromise between the positive and negative impacts of mixing on the examined process [23]. As generally acknowledged, the time has a favourable impact on the results that represent the quality of the treated wastewater, whereas it has a negative influence on those results that are associated with the cost of the treatment process. Similar results are obtained in this study.

According to Wang et al. (2023), ultrasound application in the treatment of organic wastewater utilises mechanical, thermal, and chemical effects produced through cavitation. Ultrasound's mechanical effect helps clean solid surfaces and enhances mass transfer, while its chemical and thermal effects generate OH radicals and persulfate, thereby increasing reaction rates and accelerating the breakdown of organic pollutants [59]. Considering the complexity of the mechanism of action of ultrasound, the results of Taguchi optimisation are not surprising, since they confirm that combining US with EC and zeolite, along with adjustments to US intensity, electrode material, mixing speed, and contact time, shows that synergistic and antagonistic effects are interwoven, suggesting the presence of a threshold point between them. However, additional investigation must be performed to detect the threshold point more accurately.

**Table 7.** Effect of controllable factors on the *S*/*N* ratio.

| | COD Decrease | | | | Settling Velocity | | | |
|---|---|---|---|---|---|---|---|---|
| **Factor** | **US** | **M** | **N** | **t** | **US** | **M** | **N** | **t** |
| Level 1 | 38.30 | 38.53 | 38.20 | 37.85 | 5.147 | −10.855 | −7.741 | −23.124 |
| Level 2 | 38.17 | 38.37 | 38.40 | 38.40 | −22.006 | −10.870 | −12.867 | −24.019 |
| Level 3 | 38.42 | 37.98 | 38.30 | 38.64 | −28.832 | −23.967 | −25.083 | −1.451 |
| | **Loss of Electrode mass** | | | | **Voltage** | | | |
| **Factor** | **US** | **M** | **N** | **t** | **US** | **M** | **N** | **t** |
| Level 1 | 15.49 | 19.20 | 15.88 | 19.94 | −24.94 | −24.42 | −25.46 | −25.15 |
| Level 2 | 15.92 | 17.35 | 15.41 | 14.99 | −22.41 | −23.14 | −22.04 | −23.57 |
| Level 3 | 14.86 | 9.72 | 14.98 | 11.34 | −24.75 | −25.51 | −24.60 | −23.38 |

**Table 8.** Assessment of the optimal levels and importance of a particular factor.

| | COD Decrease | | | | Settling Velocity | | | |
|---|---|---|---|---|---|---|---|---|
| **Factor** | **US** | **M** | **N** | **t** | **US** | **M** | **N** | **t** |
| Optimal level | 3 | 1 | 2 | 3 | 1 | 1 | 1 | 3 |
| pC, % | 5.81 | 29.54 | 3.65 | 61.00 | 48.32 | 8.56 | 11.87 | 31.25 |
| Rank | 3 | 2 | 4 | 1 | 1 | 4 | 3 | 2 |
| | **Loss of Electrode mass** | | | | **Voltage** | | | |
| Factor | **US** | **M** | **N** | **t** | **US** | **M** | **N** | **t** |
| Optimal level | 2 | 1 | 1 | 1 | 2 | 2 | 2 | 3 |
| pC, % | 0.64 | 56.99 | 0.45 | 41.92 | 25.64 | 21.27 | 40.82 | 12.27 |
| Rank | 3 | 1 | 4 | 2 | 2 | 3 | 1 | 4 |

## 4. Conclusions

A comprehensive evaluation of different ultrasound power settings in a triple hybrid wastewater treatment system based on electrocoagulation, zeolite, and ultrasound (EC + Z + US) was performed on compost wastewater. The results indicate that increasing the US intensity had no significant effect on solution pH, while temperature increased slightly more. The COD reduction was between 81.42 and 88.90%, whereby the best removal was achieved using iron electrodes and an ultrasonic intensity of level 2. When analysing the impact of the electrode material, a sequence of Zn < Al < Fe was observed. The best turbidity removal was achieved using iron electrodes without ultrasound and with an ultrasound intensity level 2 (98.45% and 97.95%). Optical microscope images clearly showed damage to the anodic and cathodic surfaces, mostly in the form of general and pitting corrosion. Anode consumption was visible in all experiments, especially with Zn electrodes. Changes in the mass of the cathodes were also visible, and there was an increase or decrease depending on the electrode material. Energy consumption was the lowest with Fe electrodes. When using different ultrasonic intensities, a decrease in energy consumption was observed with Al and Fe electrodes, while the opposite effect was observed with Zn electrodes. Taguchi optimisation indicated that the use of ultrasound positively influenced COD reduction and the retention of the original electrode mass, while it had a significant negative influence on settling velocity.

Since the results of this study indicate that the simultaneous application of zeolite and increased ultrasonic intensity showed no synergistic effect with respect to all parameters investigated, except for the hybrid ECZ process with Fe electrodes and 100% ultrasound power intensity, it is evident that the choice of electrode material is crucial in hybrid processes combining zeolite and ultrasound. Therefore, further studies should focus on analysing the threshold point of ultrasound intensity for each electrode material and the influence of continuous or intermittent (pulsed) ultrasonic application. Additionally, the process can be further enhanced by implementing effective filtration of the spent zeolite and improving its recovery.

**Author Contributions:** N.V.M., L.V. and S.G.: Formal analysis, Conceptualisation, Methodology, Validation, Writing—original draft, Supervision, Writing—Review and Editing. S.S.: Conceptualisation, Writing—original draft, Methodology; Modelling, Supervision, Writing—Review and Editing. I.Č.: Formal analysis, Investigation, Writing—original draft, Writing—Review and Editing. All authors have read and agreed to the published version of the manuscript.

**Funding:** The results in this paper are funded by institution funds from the Faculty of Chemical Technology University of Split, Croatia.

**Data Availability Statement:** The datasets analysed in this current study are available from the corresponding author.

**Conflicts of Interest:** The authors declare no conflicts of interest.

## References


1. Zajac, O.; Zielinska, M.; Zubrowska-Sudol, M. Enhancing wastewater treatment efficiency: A hybrid technology perspective with energy-saving strategies. *Bioresour. Technol.* **2024**, *399*, 130593. https://doi.org/10.1016/j.biortech.2024.130593.
2. Boinpally, S.; Kolla, A.; Kainthola, J.; Kodali, R.; Vemuri, J. A state-of-the-art review of the electrocoagulation technology for wastewater treatment. *Water Cycle* **2023**, *4*, 26–36. https://doi.org/10.1016/j.watcyc.2023.01.001.
3. Mao, Y.; Zhao, Y.; Cotterill, S. Examining Current and Future Applications of Electrocoagulation in Wastewater Treatment. *Water* **2023**, *15*, 1455. https://doi.org/10.3390/w15081455.
4. Roberge, P.R. *Handbook of Corrosion Engineering*, 3rd ed.; McGraw Hill: Toronto, ON, Canada, 2019.
5. Vachtsevanos, G.; Natarajan, K.A.; Rajamani, R.; Standborn, P. *Corrosion Processes Sensing, Monitoring, Data Analytics, Prevention/Protection, Diagnosis/Prognosis and Maintenance Strategies*; Springer Nature: Cham, Switzerland, 2020.
6. Svilović, S.; Vukojević Medvidović, N.; Vrsalović, L.; Midenjak, A. Treatment Efficiency of Electrocoagulatin Combined with Different Size of Natural Zeolite Particles. *Kem. Ind.* **2024**, *73*, 101–108 https://doi.org/10.15255/KUI.2023.038.
7. Ingelson, M.; Yasri, N.; Roberts, E.P.L. Electrode passivation, faradaic efficiency, and performance enhancement strategies in electrocoagulation—A review. *Water Res.* **2020**, *180*, 116433. https://doi.org/10.1016/j.watres.2020.116433.
8. Rakhmania Kamyab, H.; Yuzir, M.A.; Abdullah, N.; Quan, L.M.; Riyadi, F.A.; Marzouki, R. Recent Applications of the Electrocoagulation Process on Agro-Based Industrial Wastewater: A Review. *Sustainability* **2022**, *14*, 1985. https://doi.org/10.3390/su14041985.
9. Chow, H.; Pham, A.L.-T. Mitigating Electrode Fouling in Electrocoagulation by Means of Polarity Reversal: The Effects of Electrode Type, Current Density, and Polarity Reversal Frequency. *Water Res.* **2021**, *197*, 117074. https://doi.org/10.1016/j.watres.2021.117074.
10. Yang, Z.; Xu, H.; Zeng, G.; Luo, Y.; Yang, X.; Huang, J.; Wang, L.-K.; Song, P. The behavior of dissolution/passivation and the transformation of passive films during electrocoagulation: Influences of initial pH, Cr(VI) concentration, and alternating pulsed current. *Electrochim. Acta* **2015**, *153*, 149–158. https://doi.org/10.1016/j.electacta.2014.11.183.
11. Moradi, M.; Vasseghian, Y.; Arabzade, H.; Khaneghah, A.M. Various wastewaters treatment by sono-electrocoagulation process: A comprehensive review of operational parameters and future outlook. *Chemosphere* **2020**, *263*, 128314. https://doi.org/10.1016/j.chemosphere.2020.128314.
12. Li, J.; Song, C.; Su, Y.; Long, H.; Huang, T.; Yeabah, T.O.; Wu, W. A study on influential factors of high-phosphorus wastewater treated by electrocoagulation–ultrasound. *Environ. Sci. Pollut. Res.* **2013**, *20*, 5397–5404. https://doi.org/10.1007/s11356-013-1537-9.
13. Șenilă, M.; Neag, E.; Tănăselia, C.; Șenilă, L. Removal of Cesium and Strontium Ions from Aqueous Solutions by Thermally Treated Natural Zeolite. *Materials* **2023**, *16*, 2965. https://doi.org/10.3390/ma16082965.
14. Król, M. Natural vs. Synthetic Zeolites. *Crystals* **2020**, *10*, 622. https://doi.org/10.3390/cryst10070622.
15. Jagaba, A.H.; Kutty, S.R.M.; Hayder, G.; Latiff, A.A.A.; Aziz, N.A.A.; Umaru, I.; Ghaleb, A.A.S.; Abubakar, S.; Lawal, I.M.; Nasara, M.A. Sustainable use of natural and chemical coagulants for contaminants removal from palm oil mill effluent: A comparative analysis. *Ain Shams Eng. J.* **2020**, *11*, 951–960. https://doi.org/10.1016/j.asej.2020.01.018.
16. Abouelenien, F.; Trabik, Y.A.; Shukry, M.; El-Sharnouby, M.; Sayed, S.; Gaber, A.; Elsaidy, N.R. A Pilot Model for the Treatment of Slaughterhouse Wastewater Using Zeolite or Psidium-Leaf Powder as a Natural Coagulant, Followed by Filtration with Rice Straw, in Comparison with an Inorganic Coagulant. *Processes* **2022**, *10*, 887. https://doi.org/10.3390/pr10050887.
17. Cui, H.; Yin, L.; Huang, X.; Yu, Z.; Zhang, Z.; Dai, Z. Zeolite fly ash-enhanced coagulation treatment of oil recovery wastewater from polymer flooding. *Environ. Sci. Pollut. Res.* **2022**, *29*, 90318–90327. https://doi.org/10.1007/s11356-022-22035-7.
18. Vianney, M.J.M.; Muthukumar, K. Studies on Dye Decolorization by Ultrasound Assisted Electrocoagulation. *Clean–Soil Air Water* **2015**, *44*, 232–238. https://doi.org/10.1002/clen.201400011.
19. He, C.-C.; Hu, C.-Y.; Lo, S.-L. Evaluation of sono-electrocoagulation for the removal of Reactive Blue 19 passive film removed by ultrasound. *Sep. Purif. Technol.* **2016**, *165*, 107–113. https://doi.org/10.1016/j.seppur.2016.03.047.
20. Savun-Hekimoğlu, B. A Review on Sonochemistry and Its Environmental Applications. *Acoustics* **2020**, *2*, 766–775. https://doi.org/10.3390/acoustics2040042.
21. Al-Yaqoobi, A.; Naeemah, M.; Algharrawi, K. Treatment of dairy wastewater by electrocoagulation and ultrasonic-assisted electrocoagulation methods. Environ. *Eng. Manag. J.* **2021**, *20*, 949–957.
22. Smoković, D.; Posavčić, H.; Licht, K.; Halkijević, I. Ultrasound assisted electrocoagulation removal of heavy metals from water. In Proceedings of the 17th International Conference on Water Management and Hydraulic Engineering (WMHE 2022/Michał, Szydłowski (ur.), Sopot, Poland, 14–18 September 2022; pp. 184–190.
23. Svilović, S.; Vukojević Medvidović, N.; Vrsalović, L.; Gudić, S.; Mikulandra, A.-M. Ultrasonically Assisted Electrocoagulation Combined with Zeolite in Compost Wastewater Treatment. *Processes* **2024**, *12*, 951. https://doi.org/10.3390/pr12050951.
24. Svilović, S.; Vukojević Medvidović, N.; Vrsalović, L.; Kulić, A. Combining natural zeolite and electrocoagulation with different electrode materials–electrode surface analysis and Taguchi optimization. *Appl. Surf. Sci. Adv.* **2020**, *12*, 100330, https://doi.org/10.1016/j.apsadv.2022.100330.
25. Vukojević Medvidović, N.; Vrsalović, L.; Svilović, S.; Magaš, K.; Jozić, D.; Čović, A. Electrocoagulation Combined with Synthetic Zeolite—Does the Size of Zeolite Particles Matter? *Minerals* **2023**, *13*, 1141. https://doi.org/10.3390/min13091141.
26. Concha, A.F. Kynch Theory of Sedimentation. *Fluid Mech. Its Appl.* **2014**, *105*, 97–118.

27. Ozturk, E.; Bal, N. Evaluation of ammonia–Nitrogen removal efficiency from aqueous solutions by ultrasonic irradiation in short sonication periods. *Ultrason. Sonochem.* **2015**, *26*, 422–427. https://doi.org/10.1016/j.ultsonch.2015.02.012.
28. Wen, H.; Cheng, D.; Chen, Y.; Yue, W.; Zhang, Z. Review on ultrasonic technology enhanced biological treatment of wastewater. *Sci. Total Environ.* **2024**, *925*, 71260. https://doi.org/10.1016/j.scitotenv.2024.171260.
29. Asgharian, F.; Khosravi-Nikou, M.R.; Anvaripour, B.; Danaee, I. Electrocoagulation and ultrasonic removal of humic acid from wastewater. *Environ. Prog. Sustain. Energy* **2016**, *36*, 822–829. https://doi.org/10.1002/ep.12512.
30. Wang, J.; Wang, Z.; Vieira, C.L.Z.; Wolfson, J.M.; Pingtian, G.; Huang, S. Review on the treatment of organic pollutants in water by ultrasonic technology. *Ultrason Sonochem.* **2019**, *55*, 273–278. https://doi.org/10.1016/j.ultsonch.2019.01.017.
31. Al-Rubaiey, N.A.; Al-Barazanjy, M.G. Ultrasonic technique in treating wastewater by electrocoagulation. *Eng. Technol. J.* **2018**, *36*, 54–62. https://doi.org/10.30684/etj.36.1C.9.
32. Özyonar, F.; Gökkuş, Ö.; Sabuni, M. Removal of disperse and reactive dyes from aqueous solutions using ultrasound-assisted electrocoagulation. *Chemosphere* **2020**, *258*, 127325. https://doi.org/10.1016/j.chemosphere.2020.127325.
33. Croatian Regulation on Emission Limits Values in Wastewater, NN 26/2020 (In Croatian). Available online: https://narodne-novine.nn.hr/clanci/sluzbeni/2020_03_26_622.html (accessed on 10 September 2024).
34. Roy, D.; Azaïs, A.; Benkaraache, S.; Drogui, P.; Tyag, R.D. Composting leachate: Characterization, treatment, and future perspectives. *Rev Environ. Sci. Biotechnol.* **2018**, *17*, 323–349. https://doi.org/10.1007/s11157-018-9462-5.
35. Chatterjee, N.; Flury, M.; Hinman, C.; Cogger, C.G. *Chemical and Physical Characteristics of Compost Leachates—A Review, Report, Washington State Department of Transportation*; Washington State University: Pullman, WA, USA, 2013. Available online: https://www.wsdot.wa.gov/research/reports/fullreports/819.1.pdf (accessed on 10 September 2024).
36. Mullane, J.M.; Flury, M.; Iqbal, H.; Freeze, P.M.; Hinman, C.; Cogger, C.G.; Shi, Z. Intermittent rainstorms cause pulses of nitrogen, phosphorus, and copper in leachate from compost in bioretention systems. *Sci. Total Environ.* **2015**, *537*, 294–303. https://doi.org/10.1016/j.scitotenv.2015.07.157.
37. Rezaei, H.; Narooie, M.R.; Khosravi, R.; Mohammadi, M.J.; Sharafi, H.; Biglari, H. Humic Acid Removal by Electrocoagulation Process from Natural Aqueous Environments. *Int. J. Electrochem. Sci.* **2018**, *13*, 2379–2389. https://doi.org/10.20964/2018.03.10.
38. Koparal, A.; Yildiz, Y.; Keskinler, B.; Demircioglu, N. Effect of initial pH on the removal of humic substances from wastewater by electrocoagulation. *Sep. Purif. Technol.* **2008**, *59*, 175–182. https://doi.org/10.1016/j.seppur.2007.06.004.
39. Kourdali, S.; Badis, A.; Saiba, A.; Boucherit, A.; Boutoumi, H. Humic acid removal by electrocoagulation using aluminium sacrificial anode under influencing operational parameters. *Desalin. Water Treat.* **2013**, *52*, 5442–5453. https://doi.org/10.1080/19443994.2013.814003.
40. Mahvi, A.H.; Maleki, A.; Rezaee, R.; Safari, M. Reduction of humic substances in water by application of ultrasound waves and ultraviolet irradiation. *Iran J. Environ. Health Sci. Eng.* **2009**, *6*, 233–240.
41. Vukojević Medvidović, N.; Vrsalović, L.; Svilović, S.; Bilušić, A.; Jozić, D. Electrocoagulation treatment of compost leachate using aluminium alloy, carbon steel and zinc anode. *Appl. Surf. Sci. Adv.* **2023**, *15*, 100404. https://doi.org/10.1016/j.apsadv.2023.100404.
42. Wu, Z.; Zhao, Y.; Fan, J.; Gao, C.; Yuan, X.; Wang, G.; Zhang, Q. Dual effects of ultrasound on fabrication of anodic aluminium oxide. *Ultrason. Sonochem.* **2023**, *96*, 106431. https://doi.org/10.1016/j.ultsonch.2023.106431.
43. Gao, Z.; Cao, J.; Muhammad Muzammal, H.; Wang, C.; Sun, H.; Chong, D.; Ma, H.; Wang, Y. Ultrasound assisted large scale fabrication of superhydrophilic anodized SnOx films with highly uniformed nanoporous arrays. *Mater. Chem. Phys.* **2020**, *242*, 122540. https://doi.org/10.1016/j.matchemphys.2019.122540.
44. Paulo, V.; Neves-Araujoa, J.; Padron-Hernandeza, E. Fast and Room-temperature Synthesis of Porous Alumina Films in Ultrasonic Assisted Bath Inducing Superficial Cavitations. *Port. Electrochim. Acta* **2019**, *37*, 123–129. https://doi.org/10.4152/pea.201902123.
45. Chellam, S.; Sari, M.A. Aluminum electrocoagulation as pretreatment during microfiltration of surface water containing NOM: A review of fouling, NOM, DBP, and virus control. *J. Hazard. Mater.* **2016**, *304*, 490–501. https://doi.org/10.1016/j.jhazmat.2015.10.054.
46. Ozyonar, F.; Karagozoglu, B. Operating cost analysis and treatment of domestic wastewater by electrocoagulation using aluminium electrodes. *Pol. J. Environ. Stud.* **2011**, *20*, 173–179.
47. Ebba, M.; Asaithambi, P.; Alemayehu, E. Investigation on operating parameters and cost using an electrocoagulation process for wastewater treatment. *Appl. Water Sci.* **2021**, *11*, 175. https://doi.org/10.1007/s13201-021-01517-y.
48. Available online: https://www.indexmundi.com/commodities/?commodity=aluminum (accessed on 10 September 2024).
49. Available online: https://markets.businessinsider.com/commodities/aluminum-price (accessed on 10 September 2024).
50. Available online: https://www.sambhavpipes.com/carbon-steel-plate.html (accessed on 10 September 2024).
51. Available online: https://dang-shop.com/proizvod.aspx?sifraID=01%20a (accessed on 10 September 2024).
52. Available online: https://www.hep.hr/elektra/poduzetnistvo/tarifne-stavke-cijene-1578/1578 (accessed on 10 September 2024).
53. Kobya, M.; Hiz, H.; Senturk, E.; Aydiner, C.; Demirbas, E. Treatment of Potato Chips Manufacturing Wastewater by Electrocoagulation. *Desalination* **2006**, *190*, 201. https://doi.org/10.1016/j.desal.2005.10.006.
54. Eskibalci, M.F.; Ozkan, M.F. Comparison of conventional coagulation and electrocoagulation methods for dewatering of coal preparation plant. *Miner. Eng.* **2018**, *122*, 106–112. https://doi.org/10.1016/j.mineng.2018.03.035.
55. Moosavirad, S.M. Feasibility study of coagulation system for greywater treatment and comparison of economical effects with those of electrocoagulation in mining areas. *J. Adv. Environ. Health Res.* **2016**, *4*, 190–198.

56. Mouedhen, G.; Feki, M.; De Petris Wery, M.; Ayedi, H.F. Behavior of aluminum electrodes in electrocoagulation process. *J. Hazard. Mater.* **2008**, *150*, 124–135. https://doi.org/10.1016/j.jhazmat.2007.04.090.
57. Svilović, S.; Mužek, M.N.; Vučenović, P.; Nuić, I. Taguchi design of optimum process parameters for sorption of copper ions using different sorbents. *Water Sci. Technol.* **2019**, *80*, 98–108. https://doi.org/10.2166/wst.2019.249.
58. Graça, N.S.; Rodrigues, A.E. The combined implementation of electrocoagulation and adsorption process for the treatment of the wastewaters. *Clean Technol.* **2022**, *4*, 1020–1053. https://doi.org/10.3390/cleantechnol4040063.
59. Wang, N.; Li, L.; Wang, K.; Huang, X.; Han, Y.; Ma, X.; Wang, M.; Lv, X.; Bai, X. Study and Application Status of Ultrasound in Organic Wastewater Treatment. *Sustainability* **2023**, *15*, 15524. https://doi.org/10.3390/su152115524.